CrystEngComm

Accepted Manuscript

ROYAL SOCIETY
OF **CHEMISTRY**

www.rsc.org/crystengcomm

CrystEngComm
RSCPublishing

ARTICLE

Cite this: DOI: 10.1039/x0xx00000x

Received 00th December 2014,
Accepted 00th January 2015

DOI: 10.1039/x0xx00000x

www.rsc.org/

Three luminescent metal-organic frameworks constructed from trinuclear zinc(II) clusters and furan-2,5-dicarboxylate

Huan-Huan Li,[a] Zheng Niu,[b] Long Chen,*[ac] Hao-Bin Jiang,[a] Ya-Ping Wang,*[d] and Peng Cheng[b]

Three metal-organic frameworks based on trinuclear building blocks, isomeric α-$\{[NH_2(CH_3)_2]_2[Zn_3(FDA)_4]\cdot 2DMF\}_n$ (**1**) and β-$\{[NH_2(CH_3)_2]_2[Zn_3(FDA)_4]\cdot 2DMF\}_n$ (**2**), as well as $\{[NH_2(CH_3)_2][Zn_3(FDA)_2(\mu_2\text{-}OH)_2(\mu_3\text{-}OH)]\cdot 1.03H_2O\}_n$ (**3**) (H_2FDA = furan-2,5-dicarboxylic acid) have been obtained under solvothermal conditions by adjusting the anions of zinc salts and solvents. These compounds are characterized by single crystal X-ray diffraction, thermogravimetric analysis and luminescent measurements. The building blocks of three MOFs are trinuclear clusters stabilized by carboxylic groups, and the resulting three-dimensional frameworks are differentiated by the structural nature of the secondary building units (SBU). MOFs **1** and **2** display ***pcu*** and ***bcu*** nets, respectively. MOF **3** exhibits a new topology, which is a 3,8-connected net with the point symbols of $(3.4.5)_2(3^4.4^4.5^2.6^6.7^{10}.8^2)$. The photoluminescence spectra of **1-3** are reported for the first time, and all the Zn(II) complexes emit blue luminescence.

Introduction

MOFs are a kind of highly useful materials for gas storage, ion separation, catalysis and luminescence, due to their various topologies, high surface areas, well-defined porosity and tunable chemical functionalities.[1-4] Luminescent MOFs exhibit intriguing properties in tunable luminescence, direct white-light emissions, and light-emitting devices.[5] Compared with conventional inorganic luminescent materials, the luminescent MOF materials have distinct advantages due to special incorporation of inorganic and organic building blocks, tunable and highly ordered structures, and functional channels. For example, luminescence generated from MOFs containing lanthanide ions is governed by various selection rules, often leading to weak and long-lived emission on the millisecond timescale. Both the metal and the linker can be used to create luminescence, and can further interact *via* "antenna effects" to increase the quantum efficiency of otherwise weakly emitting lanthanide ions. Luminescence from MOFs containing transition-metal ions is typically centered on the linker rather than on the metal. However, charge transfer between the metal and linker is also involved. Therefore, MOFs based on transition metal can exhibit luminescence on the microsecond or even nanosecond timescale.[6]

In order to construct new functional luminescent MOFs with different structures and topologies, the crucial step is to choose and design multifunctional organic ligands with suitable coordination sites and specific symmetries. Furan-2,5-dicarboxylic acid (H_2FDA) with special C_2-like symmetry has been adopted as ligands to generate highly ordered porous structures.[7,8] Moreover, H_2FDA has a strong "antenna effect", which can effectively sensitize the luminescence lanthanide ions such as Dy(III) and Tb(III) in MOFs.7[c,d] For example, in previous work, we reported a robust microporous Tb-MOF with 1D honeycomb-type channels based on H_2FDA, which showed a potential use for sensing small-molecule pollutants such as benzene and acetone.[7c] However, to the best of our knowledge, there are only a few reports on the luminescent properties of MOFs constructed from transition-metal ion such as Zn(II) or Cd(II) ions with furan-2,5-dicarboxylate.[9] In addition, the framework structures of the MOFs can be influenced by several important factors in the synthesis process, such as solvent, anion, pH, and temperature.[10] Thus, it is possible to control the final structures of the products by adjusting these factors and to obtain a wide variety of MOFs with different functions.

For this purpose, three Zn-MOFs based on trinuclear SBUs, isomeric α-$\{[NH_2(CH_3)_2]_2[Zn_3(FDA)_4]\cdot 2DMF\}_n$ (**1**), β-

$\{[NH_2(CH_3)_2]_2[Zn_3(FDA)_4]\cdot 2DMF\}_n$ (**2**) and $\{[NH_2(CH_3)_2][Zn_3(FDA)_2(\mu_2\text{-}OH)_2(\mu_3\text{-}OH)]\cdot 1.03H_2O\}_n$ (**3**) were successfully obtained *via* adjusting the anions of zinc salts and solvents. The topological variations of the compounds were studied in detail. Furthermore, the luminescent properties of Zn-MOFs with furan-2,5-dicarboxylate were investigated.

Experimental section

Materials and general methods. The H_2FDA ligand was purchased from Sigma-Aldrich Company, and other chemicals purchased were of reagent grade and used without further purification. Elemental analyses (C, H and N) were performed on a Perkin-Elmer 240 CHN elemental analyzer. IR was recorded on a Bruker TENOR 27 spectrophotometer in the range 400-4000 cm^{-1} using KBr pellets. TGA were performed on a Labsys NETZSCH TG 209 Setaram apparatus with a heating rate of 10°C/min in the nitrogen atmosphere. PXRD measurements were recorded on a D/Max-2500 X-ray diffractometer using Cu Kα radiation. The fluorescent spectrum was measured on a Varian Cary Eclipse Fluorescence spectrophotometer.

Synthesis of α-$\{[NH_2(CH_3)_2]_2[Zn_3(FDA)_4]\cdot 2DMF\}_n$ (1). A mixture of $ZnCl_2$ (0.0273 g, 0.2 mmol), H_2FDA (0.0156 g, 0.1 mmol), 2.5 mL CH_3CN and 2.5 mL DMF was sealed in a glass vial of dimensions 10 mm (outer diameter), 8 mm (inner diameter), and 150 mm (length), which was heated at 100 °C for 3 days. After slowly cooling to room temperature over an additional 3 days, colorless crystals (56% yield based on Zn) were collected after washing with DMF and dried in air. Elemental analysis for $C_{34}H_{38}N_4Zn_3O_{22}$: Calcd(%): C, 38.86; H, 3.65; N, 5.33. Found (%): C, 38.58; H, 3.89; N, 5.36. IR (KBr, cm^{-1}): 3123 (br), 1623 (s), 1351 (s), 1019 (s), 967 (m), 834 (w), 786 (s).

Synthesis of β-$\{[NH_2(CH_3)_2]_2[Zn_3(FDA)_4]\cdot 2DMF\}_n$ (2). **2** is the isomer of **1**, which has the same molecular formula. The synthetic procedure was similar to that of **1** except that $ZnCl_2$ was replaced by $ZnBr_2$ (0.0450g, 0.2 mmol). Colorless crystals (60% yield based on Zn) were obtained after washing with DMF and drying in air. Elemental analysis for $C_{34}H_{38}N_4Zn_3O_{22}$: Calcd(%): C, 38.86; H, 3.65; N, 5.33. Found (%): C, 38.78; H, 3.81; N, 5.56. IR (KBr, cm^{-1}): 3127 (br), 1613 (s), 1575 (m), 1470 (m), 1349 (s), 1016 (w), 965 (w), 804 (s), 526(w).

Synthesis of $\{[NH_2(CH_3)_2][Zn_3(FDA)_2(\mu_2\text{-}OH)_2(\mu_3\text{-}OH)]\cdot 1.03H_2O\}_n$ (3). A mixture of $ZnCO_3\cdot 2Zn(OH)_2\cdot H_2O$ (0.0684 g, 0.2 mmol), H_2FDA (0.0156 g, 0.1 mmol), 4 mL DMF and 1 mL H_2O was sealed in the same glass vial, which was also heated at 100 °C for 3 days. After slowly cooling to room temperature over an additional 3 days, colorless crystals (46% yield based on Zn) were collected after washing with DMF and dried in air. Elemental analysis for $C_{14}H_{17.068}NZn_3O_{14.034}$: Calcd(%): C, 27.12; H, 2.77; N, 2.26. Found (%): C, 27.26; H, 2.81; N, 2.52. IR (KBr, cm^{-1}): 3369 (br), 1586 (s), 1419 (m), 1379 (s), 1035 (w), 967 (w), 786 (s), 608 (w), 501 (w).

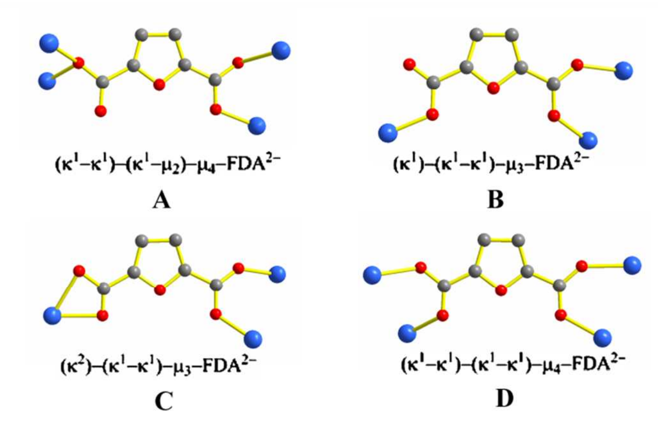

Scheme 1. Coordination mode of the H_2FDA ligand in compounds **1–3**.

Crystallographic Studies. Data collections of **1-3** were performed on a Supernova diffractometer (Agilent) at 120 K with a graphite-monochromated Mo-Kα radiation (λ = 0.71073 Å) using the ω-scan technique. CrysAlisPro program was used to process the data. The crystal was kept at 120 K during data collection. Using Olex2,[11] the structure was solved with the ShelXS structure solution program using Direct Methods and refined with the ShelXL refinement package using Least Squares minimisation.[12] The selected crystal parameters, data collection and refinements are summarized in Table S1. The selected bond lengths and angles are listed in Table S2. CCDC reference numbers of **1-3** are 1036655, 1036654 and 1023610, respectively.

Results and discussion

Synthesis. In this reaction system, several important factors can significantly influence the final structures of the products, such as solvent and anion. Three Zn-MOFs involving trinuclear building blocks are obtained after changing the anion and solvent conditions. Reaction of H_2FDA with $ZnCl_2$ in DMF/CH_3CN solution at 100°C affords colorless crystals of **1**, which shows a 3D structure of open channels along the [1,0,0], [0,1,0], and [0,0,1] directions with dimensions ~5.6 × 5.5 Å^2, ~5.0 × 3.4 Å^2, and ~9.3 × 3.9 Å^2, respectively. After changing the Cl^- to Br^-, **2** is obtained and exhibits a 3D structure with two types of open channels along the [1,0,0] direction: one is with window dimensions of 6.2 × 7.8 Å^2, and the other is with window dimensions of 6.3 × 7.7 Å^2. When $ZnBr_2$ and CH_3CN are replaced by $ZnCO_3\cdot 2Zn(OH)_2\cdot H_2O$ and H_2O in the reaction system, respectively, colorless crystals of **3** are obtained. Compared with the linear trinuclear nodes of **1** and **2**, **3** shows triangle trinuclear nodes. Moreover, the 3D framework of **3** exhibits 1D quadrangle channels along the [0,0,1] direction with dimensions ~11.0 × 11.0 Å^2. In addition, the topologies of the three compounds are different, which is attributed to the different connections of the SBUs. Further discussion will be presented below.

Description of the crystal structures. Single-crystal Xray diffraction study shows that **1** crystallizes in monoclinic space group of $P2_1/c$. There are two independent Zn(II) ions in the asymmetric unit (Fig. S1). The Zn1 center is four-coordinated to form a distorted tetrahedral geometry, where four oxygen atoms are from one μ_1-η^0:η^1 carboxylate, one μ_2-η^0:η^2 carboxylate and two different μ_2-η^1:η^1 carboxylates of four FDA ligands. The Zn2 center is six-coordinated to form a distorted octahedral coordination geometry, where six oxygen atoms are from four different μ_2-η^1:η^1 carboxylates and two different μ_2-η^0:η^2 carboxylates of six FDA ligands. There are two types of FDA^{2-}, which adopt the coordination modes A and B (Scheme 1).

Zn−O bonds possess an average distance of ~2.118 Å, which is consistent with the reported values.[7b] One Zn1 ion is linked with two Zn2 ions *via* carboxylate bridges to form a trinuclear cluster (Zn1···Zn2 ~3.328 Å). As shown in Fig. 2a, Zn_3 clusters are connected by eight FDA^{2-} to assemble into a 3D framework. The 3D framework exhibits open channels along the [1,0,0], [0,1,0], and [0,0,1] directions with dimensions ~5.6 × 5.5 $Å^2$, ~5.0 × 3.4 $Å^2$, and ~9.3 × 3.9 $Å^2$, respectively (Fig. 1), and are occupied by DMF molecules and $[NH_2(CH_3)_2]^+$ cations. PLATON analysis reveals that the 3D porous structure is composed of large voids of 2336.1 $Å^3$ that represents 55.6% per unit cell volume without guest molecules/cations.[13]

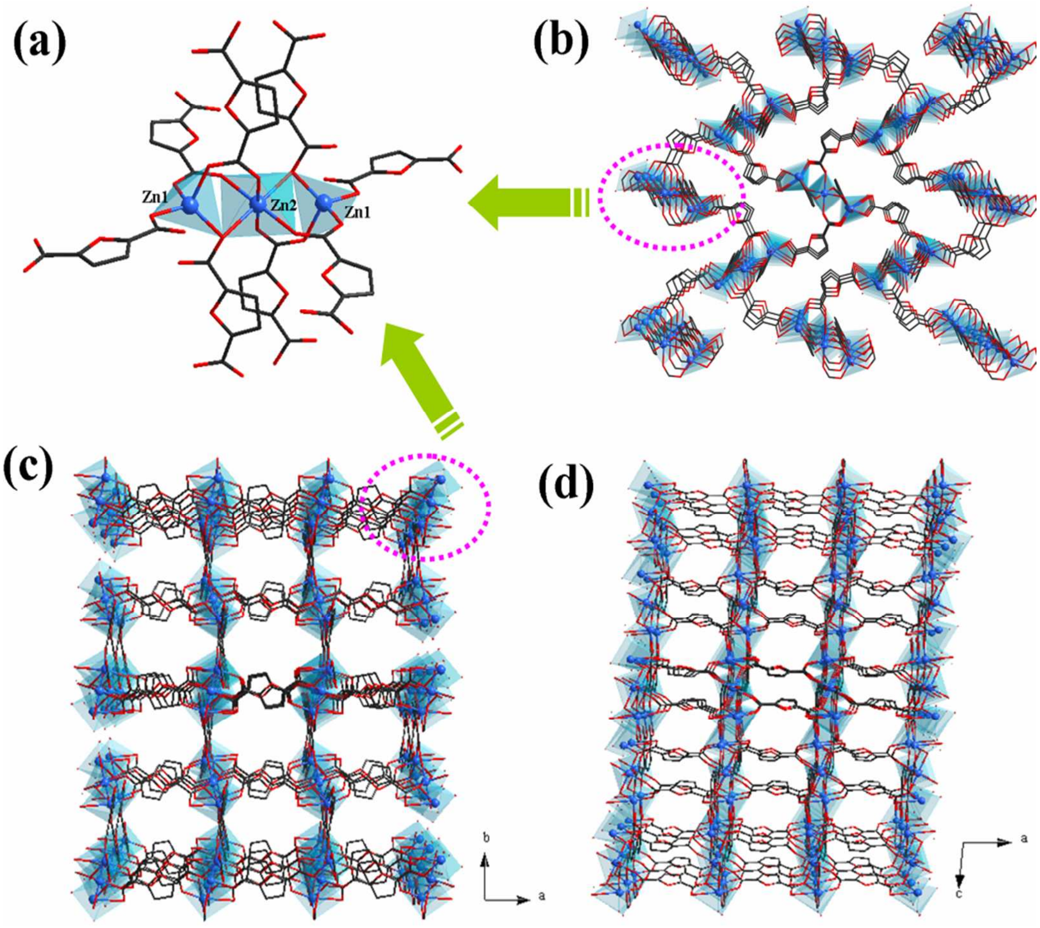

Fig. 1. Crystal structure of **1**: (a) the coordination environment of Zn(II) ions; the 3D framework view of the structure along the [1,0,0] (b), [0,1,0] (c), [0,0,1] (d) directions. Zn is in blue, O in red, and C in gray.

When replacing $ZnCl_2$ by $ZnBr_2$, MOF **2** is obtained, which is an isomer of **1** and has a biporous 3D structure. As shown in Fig. S2, **2** crystallizes in triclinic space group of *P*-1, and has four independent Zn(II) ions in the asymmetric unit. The Zn1 center is five-coordinated to form a distorted trigonal bipyramidal (tbp) geometry, where five oxygen atoms are from two different μ_2-η^1:η^1 carboxylates, one μ_2-η^0:η^2 carboxylate and one bidentate chelating μ_2-η^1:η^1 carboxylate of four FDA ligands; The Zn3 center is four-coordinated to form a distorted tetrahedral geometry, where four oxygen atoms are from one μ_1-η^1:η^0 carboxylate and three different μ_2-η^1:η^1 carboxylates of four FDA ligands. Zn2 and Zn4 are both six-coordinated to form a distorted octahedral coordination geometry. They have similar coordination environments, only one oxgen from μ_2-η^1:η^1 carboxylate becomes from μ_2-η^0:η^2 carboxylate. Compared with **1**, **2** contains two types of Zn trimeric units ({$[Zn1]_2[Zn4]$} (Zn1···Zn2 ~3.244 Å) and {$[Zn3]_2[Zn4]$} (Zn3···Zn4 ~3.580 Å). After changing the anion from Cl^- to Br^-, the tetrahedral Zn1 of the trimeric unit of **1** is transformed to distorted ***tbp*** geometry in one unit (Fig. 2a) and remains tetrahedral geometry (Zn2) in another unit in **2** (Fig. 2b).

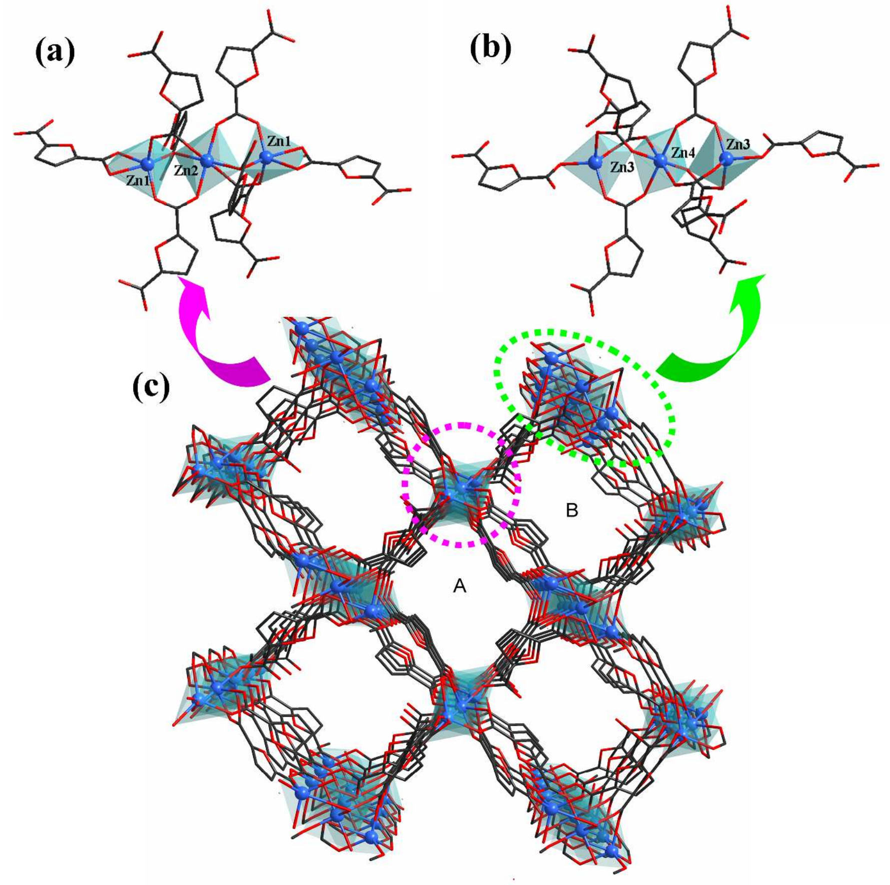

Fig. 2. (a,b) Two different coordination environment of trinuclear Zn(II) ions SBUs; (c) The 3D framework of **2** view of the structure along the [1,0,0] direction.

The Zn1 and Zn2 are connected by two μ_2-η^1:η^1 bridging carboxylates and one μ_2-η^0:η^2 carboxylate; whereas the Zn3 and Zn4 have similar connection, only μ_2 bridging carboxylate changes to bidentate carboxylate bridging. These three types of trimeric units are connected by eight FDA ligands, which adopt the coordination modes A, B and C to form a 3D structure (Scheme 1, Fig. 2c). The 3D framework exhibits two types of open channels along the [1,0,0] direction: A-type channels have dimensions of 6.2 × 7.8 Å^2 and B-type channels have dimensions of 6.3 × 7.7 Å^2, respectively. Both channels are occupied by disordered DMF molecules and $[NH_2(CH_3)_2]^+$ cations. The PLATON analysis reveals that the 3D porous structure is composed of large voids of 2234.9 Å^3 that represents 46.2% per unit cell volume without guest molecules/cations (Fig. S4).[13]

Compared with the framework structures reported previously,[7b] **1** and **2** have different voids and porosities due to the different reaction conditions and solvent. In addition, the air dried samples of **1** and **2** are more stable according to the PXRD patterns analysis. Unlike reported compounds transforming to new unknown phases when dried in the air, the diffraction peaks of the dried **1** and **2** are well in agreement with the simulated data (Fig. S1a-b). This may be due to the stronger hydrogen-bonding interaction and the steric hindrance among $[NH_2(CH_3)_2]^+$ cations, solvent molecules and framework in **1** (N3−H3A···O11, ~2.132 Å) and **2** (N2-H2A···O21, ~1.896 Å, N2-H2B···O17, ~2.129 Å and N4-H4A···O20', ~2.167 Å). Thus, the solvent molecules are hard to lose, which can continuously support the framework structures.

When replacing $ZnBr_2$ with $ZnCO_3 \cdot 2Zn(OH)_2 \cdot H_2O$ salt, and changing DMF/CH_3CN solvent to DMF/H_2O in the reaction system, **3** is obtained. Compared with **1** and **2**, **3** crystallizes in monoclinic space group *C*2/c and the framework is reported for the first time. The asymmetric unit of **3** contains two independent Zn(II) ions, one FDA^{2-} ligand, one μ_2-OH$^-$ oxygen and half μ_3-OH$^-$ oxygen atom. As shown in Fig. S3, Zn1 is five-coordinated, where three oxygen atoms are from three different μ_2-η^1:η^1 carboxylates of three FDA^{2-}, one oxygen atom is from μ_2-OH$^-$ oxygen and one oxygen atom is from μ_3-OH$^-$ oxygen. Zn2 is also five-coordinated by two oxygen atoms from two different μ_2-η^1:η^1 carboxylates of two FDA^{2-}, two oxygen atoms from μ_2-OH$^-$ and one from μ_3-OH$^-$ oxygen atom. The coordination polyhedrons of both Zn1/Zn2 show a distorted ***tbp*** geometry configuration. There is only one type of FDA^{2-}, which adopts the coordination modes D (Scheme 1). The Zn1−O bond lengths vary from 1.946(12) to 2.168(5) Å and possess an average distance of ~2.055 Å, whereas the Zn2−O bond lengths vary from 1.865(5) to 2.029(6) Å and possess an average distance of ~1.945 Å. These are consistent with the reported values.[7b]

CrystEngComm
RSCPublishing

ARTICLE

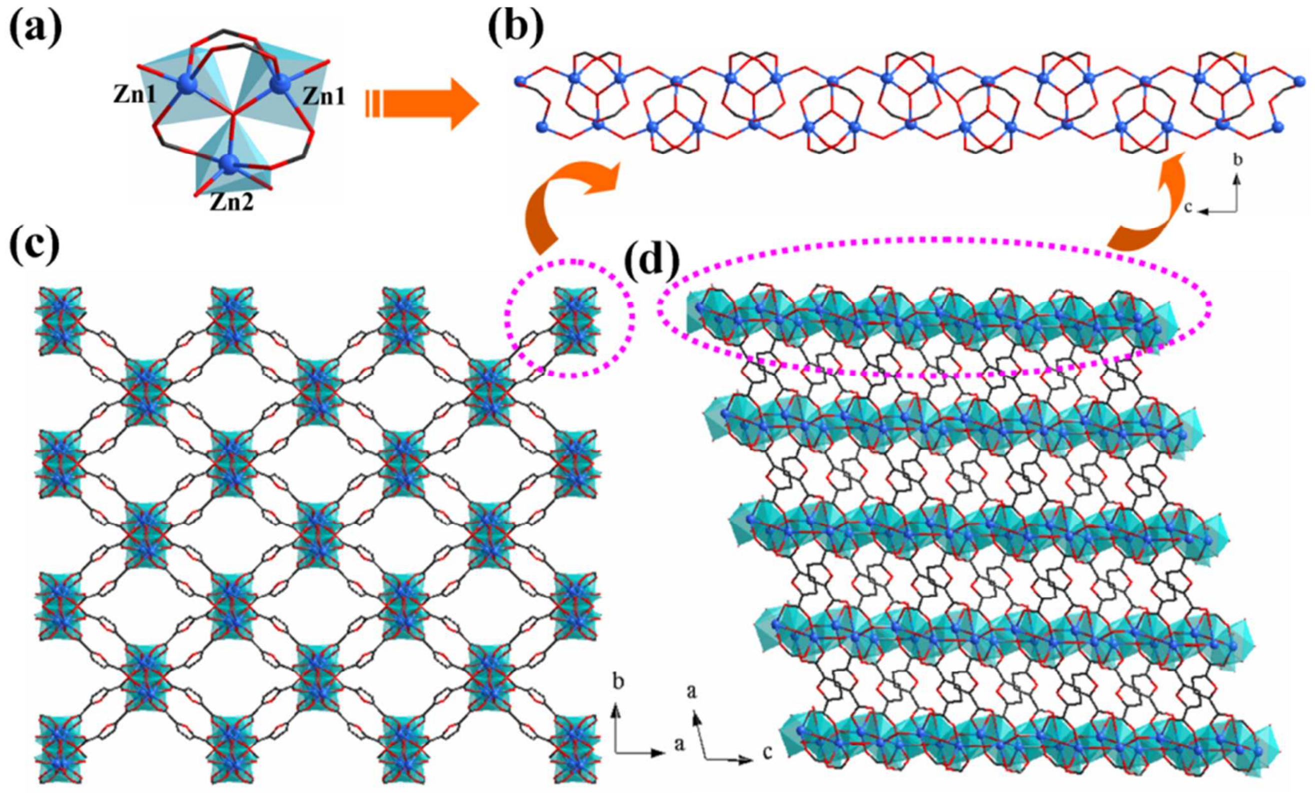

Fig. 3. Crystal structure of **3:** (a) Trinuclear $[Zn_3\text{-}(\mu_3\text{-}OH)]^{5+}$ clusters; (b) 1D $\{[Zn_3\text{-}(\mu_3\text{-}OH)(\mu_2\text{-}OH)_2](COO)_2\}_n$ chain; the 3D framework of **3** view along (c) [0,0,1] and (d) [0,1,0] directions.

As shown in Fig. 3a, on one hand, two Zn1 are linked with each other *via* two $\mu_2\text{-}\eta^1\text{:}\eta^1$ carboxylate bridges. The distance of Zn1···Zn1 is ~3.345 Å and the angle of Zn1-O7-Zn1 is 111.707°. On the other hand, Zn1 and Zn2 are linked *via* one $\mu_2\text{-}\eta^1\text{:}\eta^1$ carboxylate bridge and one $\mu_2\text{-}OH_2$ oxygen with Zn1-Zn2 distance of ~3.353 Å and Zn1-O-Zn2 angle of 117.962°. Finally, the $\mu_3\text{-}OH^-$ oxygen group holds Zn1 and Zn2 atoms together to form a triangle trinuclear $[Zn_3\text{-}(\mu_3\text{-}OH^-)]^{5+}$ cluster that acts as a node in the 3D network. Each cluster is supported by four $\mu_2\text{-}\eta^1\text{:}\eta^1$ carboxylate groups of FDA^{2-}, four $\mu_2\text{-}OH^-$ oxygen atoms and is connected to each other through two $\mu_2\text{-}OH^-$ groups to form a 1D chain (Fig. 3b). These 1D chains are cross linked *via* the FDA^{2-} ligands to generate a 3D framework (Fig. 3c-e). The 3D framework exhibits 1D quadrangle channels along the [0,0,1] direction with dimensions ~11.0 × 11.0 Å^2, occupied by DMF molecules (Fig. 3f). PLATON analysis reveals that the 3D porous structure contains large voids of 38.0 % that represents 2264.8 Å^3 per unit cell volume when the guest molecules are removed (Fig.S5).[13]

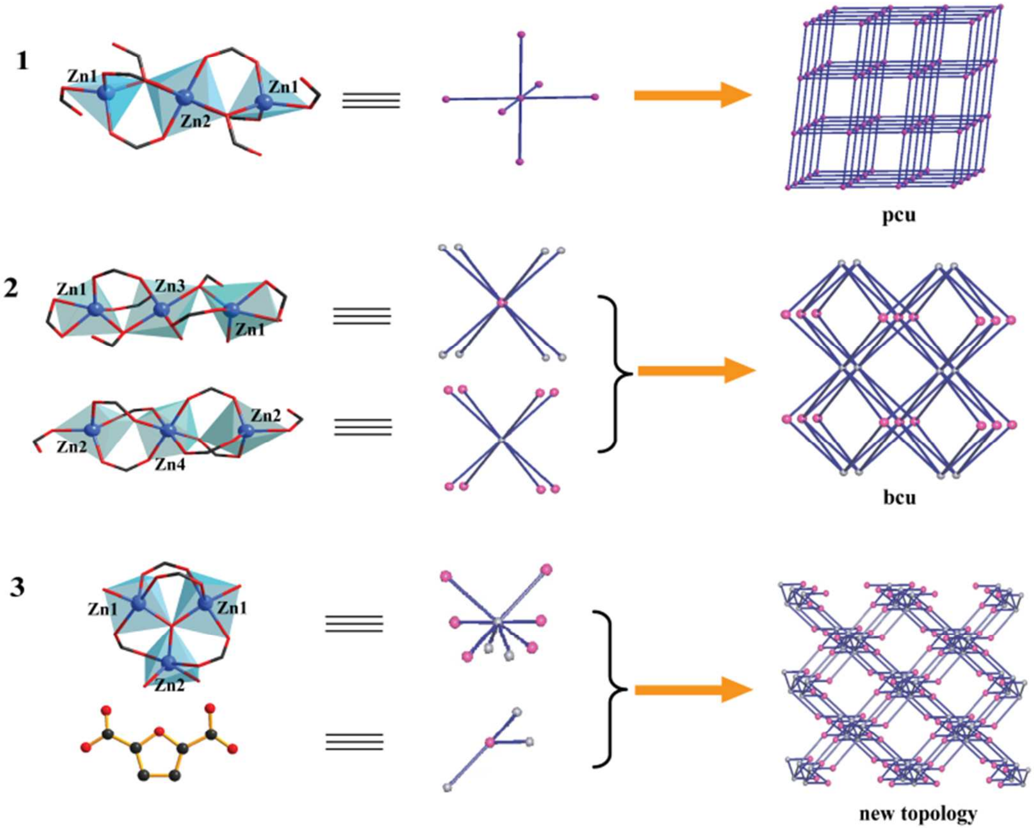

Scheme 2. Simplified topological structure of **1-3**. The pink nodes represent the trinuclear SBU in **1-2**, light gray nodes represent the another trinuclear SBU in **2** and FDA^{2-} nodes in **3**, respectively.

Further research on the nature of the frameworks can be achieved by the application of a topological approach, and topology analysis for **1-3** by freely available program TOPOS and systre for the first time.[14] As shown in Scheme 2, for **1**, if the trinuclear Zn_3 clusters are considered as uninodal-connected nodes and the FDA^{2-} are considered as bridging spacers, the entire structure can be simplified as a six-connected ***pcu*** net.[15] The point symbol for **1** is $(4^{12}.6^3)$. For **2**, if {[Zn1]$_2$[Zn2]} trinuclear SBU is considered as a 8-connected node, {[Zn3]$_2$[Zn4]} trinuclear SBU is considered as another 8-connected node, and the FDA^{2-} serve as bridging linkers (Scheme 2), this structure can be considered as a two nodes 8,8-connected net named ***bcu*** body centered cubic. Actually, although the structure of ***bcu*** net is commonly found in textbooks, such 2-node topology with 8-connected nodes in a cubic geometry is extremely rare in MOFs owing to severe geometric requirements.[16] The point symbol of the topology can be expressed as $(4^{24}.6^4)$. For **3**, if the trinuclear Zn_3 clusters are considered as 8-connected nodes and some of FDA^{2-} serve as 3-connected node while others as bridging linkers to link Zn_3 SBUs, the entire structure can be simplified as a 2-nodes 3,8-connected net. The point symbol for **3** is $(3.4.5)_2(3^4.4^4.5^2.6^6.7^{10}.8^2)$. This is a unique topology and has not been observed in MOF chemistry previously.[15]

Apart from this, the six-connections such as ***pcu*** net are commonly and easily synthesized for Zn-MOFs constructed from dicarboxylic acid with C_2-like symmetry such as pyridine-2,6-dicarboxylic acid (H_2PDA), thiophene-2,5-dicarboxylic acid (H_2TDC), terephthalic acid and isophthalic acid. There are few reports on the constructing of Zn-MOFs with eight-connections, largely due to the conformation of the ligands (such as the angles between two carboxyl groups and coordination abilities of coordination groups).[17] Recently, three Zn-MOFs (Zn-**1**, Zn-**2** and Zn-**3**) based on H_2TDC *via* organic cation templated are obtained,[18] which show ***bcg***, ***bcu*** and ***flu*** net, respectively. On one hand, H_2FDA is similar to H_2TDC except for oxygen atom instead of sulfur atom. Thus, they may generate similar structures such as eight connections net. For example, both **2** and Zn-**2** have ***bcu*** net. On the other hand, compared with H_2TDC, oxygen atom of H_2FDA is smaller than sulfur atom. So the two carboxylic groups are closer, leading to their own characteristics net. A comparison of **1-3** with Zn **1-3** suggests that the conformation of dicarboxylate ligand dictates the resulting structures.

In all, according to the topological analysis results, adjusting anion of the metal salts and tuning solvent based on H_2FDA ligand in the reaction system can effectively control the topology of the frameworks.

TGA and PXRD analyses. To confirm the phase purity of **1-3**, the PXRD patterns have been collected (Fig. S6). The diffraction peaks of the as-synthesized samples are well in agreement with the calculated data, demonstrating the high phase purity of the compounds. TGA of **1-3** are performed in the temperature range of 25-600 °C, as shown in Fig.S7. The TGA of **1** shows an initial weight loss of 13.1% from 25 to 210 °C, corresponding to the loss of two guest DMF molecules (calcd 13.9 %). Then, **1** decomposed vigorously at a temperature higher than 300 °C. **2** has similar thermal performance to **1**. It loses 14.8% weight in the range of 25−180°C, corresponding to the release of one lattice guest DMF molecule (calcd 13.9 %), and also begins to decompose at a temperature up to 300°C. The TGA of **3** indicates an initial weight loss of 4.9 % from 25 to 200 °C, corresponding to the loss of guest water molecules (calcd 4.5 %). Upon further heating, it decomposes vigorously at temperature higher than 350 °C.

Luminescence properties. As is well known, the d^{10} transition metal compounds exhibit changeable luminescence behaviors. The emission wavelength and luminescence mechanism can be significantly affected by organic ligands and their coordination modes.[19]

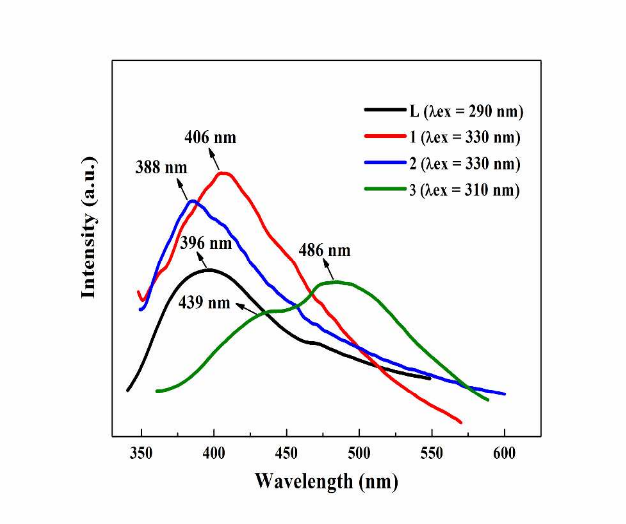

Fig. 4. Solid-state excitation (black line) and emission (red line) spectra of H_2FDA (a) and **1-3** (b-d) at room temperature.

The photoluminescent spectra of **1-3** and the free ligands H_2FDA are measured for the first time at room temperature (Fig. 4). The emission spectra for the free ligand H_2FDA and **1-2** show a single peak at 396 nm with λex = 290 nm, 406 nm and 388 nm with λex = 330 nm, respectively. The emission spectrum for **3** shows a main peak at 485 nm and a shoulder peak at 439 nm with λex = 310 nm. The above results reveal that the peaks of the emission spectra for **1-2** are very closed to that of the free ligand, which can probably be attributed to the intraligand fluorescent emission of π*–π transitions of metal coordinated H_2FDA.[20]

In addition, although d^{10} Zn(II) ions are difficult to be oxidized or reduced which result in metal-to-ligand charge transfer (MLCT) or ligand-to-metal charge transfer (LMCT), respectively, and often exhibit ligand-centered emission, the LMCT phenomenon can be occasionally observed in Zn(II) complexes.5[,21,22] For **3,** the main peak with a significant red-shift compared to H_2FDA may be assigned to the ligand-to-metal charge-transfer (LMCT) bands due to the special Zn(II) ions coordination environments, the trizinc Zn_3-(μ_3-OH) cores and 1D $\{[Zn_3\text{-}(\mu_3\text{-OH})(\mu_2\text{-OH})_2]_n$ chains of the structure. A Zn-MOF with similar Zn(II) ions coordination environment was reported previously,[21] which is also constructed with the $Zn_3(\mu_3\text{-OH})$ cores, and the cores are further interlinked *via* the μ_3-OH groups to generate a helical $[Zn_3(\mu_3\text{-OH})(\mu_2\text{-OH})]_n$ chain. Such a structure shows a maximum peak at 422 nm upon excitation at 325 nm, which is also attributable to the ligand-to-metal charge transfer (LMCT).[21,22] The shoulder peak of the emission spectrum of **3** probably arises from the free ligands H_2FDA, which are attributed to the π*–π transitions[20] Therefore, the luminescence properties of **1-3** are in accord with the most reported Zn-MOFs (Table 1).

Table 1. Solid-state excitation and emission wavelengths and mechanism of **1-3** and selected Zn-MOFs[a].

Compound	λex (nm)	λem (nm)	Mechanism	Ref.
1	330	406	Linker-based	*This work*
2	330	388	Linker-based	*This work*
3	310	439, 486	LMCT	*This work*
$\{[Zn_7(OH)_8(DTA)_3]\cdot H_2O\}_n$		483	Linker-based	23a,b
$[Zn_3(TCPB)_2(H_2O)_2]\cdot 2H_2O\cdot 4DMF$	~375	~450	Linker-based	23c
$\{[Zn_2(L^1)(4\text{-}abpt)(H_2O)_3]\cdot 5H_2O\}_n$	275	~449	LMCT	22
$\{[Zn_2(L^2)(4\text{-}abpt)(H_2O)]\cdot 2.5H_2O\}_n$	275	~369; 452	Linker-based, LMCT	22
$\{[Zn_{1.5}(HL^2)(3\text{-}abpt)(H_2O)]\cdot H_2O\}_n$	275	347	Linker-based	22
$\{[Zn(tipa)Cl]\cdot NO_3\cdot 2DMF\}_n$	365	414 (298K)	Linker-based	6a
$[Zn_7(TMBHB)_2\cdot 2NO_3\cdot 5DMF\cdot 4CH_3CH_2OH\cdot 6H_2O]_n$	300	393	Linker-based	24a
$[Zn(NH_2bdc)(bix)\cdot(DMF)_2]_n$	380	426	LMCT	24b
$[Zn_3(cpoip)_2(4,4'\text{-}bpy)\cdot 2H_2O]$	377	448	The Zn–O inorganic cluster	25a
$[Zn_2(tzba)(DMF)]\cdot 0.5DMF$	325	413	LMCT	25b
$[Zn(bpmb)(HCOO)]_n\cdot[Zn(bpmb)(OH)]_n\cdot 4nH_2O$	377	431	Linker-based	25c
$[Zn_2(bpmb)(1,3,5\text{-}btc)]_n\cdot nDMA$	377	429	Linker-based	25c
$[Zn_5(\mu_3\text{-OH})_2(BTA)_2(tp)_3]_n$	260	348	Linker-based; LMCT	26a
$[Zn(BTA)(chdc)0.5]n$	287	380	Linker-based; LMCT	26a
$[Zn(BTA)(ap)0.5]n$	264	360	Linker-based; LMCT	26a
$[Zn_3(btrc)_2(L1)]_n$	350	399	LMCT	26b
$[Zn(LTP)_2]_n$	370	458	Linker-based; LMCT	26c
$Zn_3L_3(DMF)_2$	350	396, 420, 441	Linker-based; sensing, scintillation	5, 26d
$[Zn_3(\mu_3\text{-OH})(\mu_2\text{-OH})(4,4'\text{-}bpy)_{0.5}(4,4'\text{-}oba)_2]\cdot 0.5H_2O$	325	422	LMCT	21

[a] Linker (common name): DTA^{2-} = 9,10-ditetrazolateanthracene; H_3TCPB=1,3,5-tri(4-carboxyphenoxy)benzene; H_4L^1 = 5,5'-(1,4-phenylenebis(methoxy))diisophthalic acid; 4-abpt = 4-amino-3,5-bis(4-pyridyl)-1,2,4-triazole; H_4L^2 = 5,5'-(1,3-phenylenebis(methoxy))diisophthalic acid; 3-abpt = 4-amino-3,5-bis(3-pyridyl)-1,2,4-triazole; tipa = tri(4-imidazolylphenyl)amine; H_6TMBHB = 3,3',3'',5,5',5''-benzene-1,3,5-triylhexabenzoic acid; bix = 1,4-bis(imidazol-1-ylmethyl)benzene; H_3pcoip = 4-(2-carboxyphenoxy)isophthalic acid; 4,4'-bpy = 4,4'-bipyridine; H_2tzba = 4-(1H-tetrazol-5-yl) benzoic acid; Hbpmb = 3,5-bis(4-pyridylmethoxy)benzoic acid; 1,3,5-H_3btc = 1,3,5-benzenetricarboxylic acid; DMA = N,N-dimethylacetamide; BTAH = benzotriazole; H_2tp = terephthalic acid, H_2chdc= 1,4-cyclohexanedicarboxylic acid, H_2ap = adipic acid, H_3btrc=1,2,4-benzenetricarboxylic acid; L1 = 1, 3-bis(4-pyridyl)propane); LTP = L-thioproline; L = trans-4,4'-Stilbenedicarboxylic acid; 4,4'-oba = 4,4'-oxybis(benzoate).

Furthermore, the luminescence investigations mentioned above demonstrated that H_2FDA is a good candidate for enhanced emissive properties, tunable, in principle by coordination to different metals or environment, which can effectively sensitize not only the luminescence lanthanide ions according to our previous works,[7c,7d] but also the luminescence of the transition metal Zn(II) ions. The difference among the luminescent properties of the three compounds can be ascribed to the different coordination environment of Zn(II) ions.[22] For instance, Zn(II) ions have similar coordination environment in **1**-**2**, so they have similar luminescent properties as compared to **3**. Moreover, as shown in Fig. 5, the CIE chromaticity of the compounds exhibit blue luminescence, which may be considered as promising candidates for the exploration of fluorescent materials.

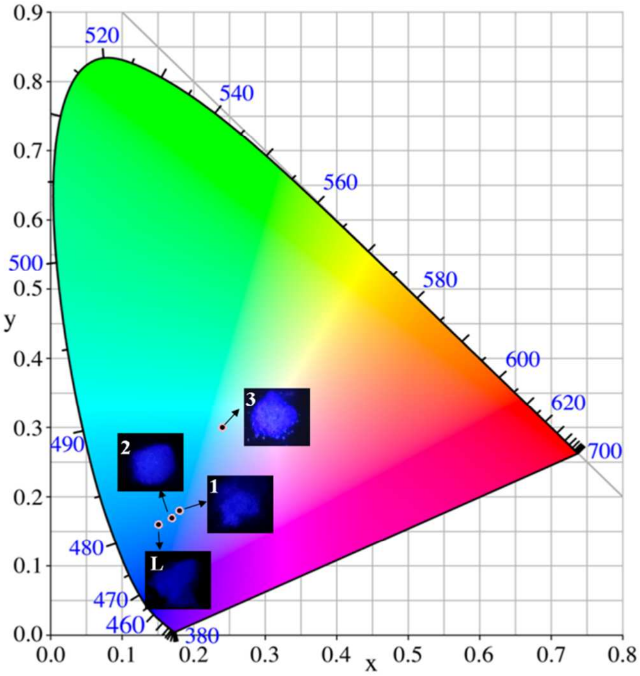

Fig. 5. The CIE chromaticity of **1**-**3** and H_2FDA (L).

Conclusions

In summary, we have successfully synthesized three Zn-MOFs based on trinuclear nodes with furan-2,5-dicarboxylic acid *via* solvothermal conditions. The topology controlled was obtained by a tuning strategy which was attributed to the changes in the local coordinate environment around the Zn centers. Topological and luminescence analysis of **1**-**3** were taken for the first time. **1** and **2** exhibited ***pcu*** and ***bcu*** net, respectively; whereas **3** exhibited a unique 3,8-connected net topology with the point symbol of $(3.4.5)_2(3^4.4^4.5^2.6^6.7^{10}.8^2)$. Furthermore, **1**-**3** also displayed significant blue luminescence. Further studies on the luminescence properties of d^{10} transition metal MOFs constructed with furan-2,5-dicarboxylic acid are under way.

Acknowledgements

We thank "973 Program" (2011CB013000), the NSF of Jiangsu Province (BK2012293, BK20130482), the University Natural Science Research Project of Jiangsu Province (13KJB430008), Research Foundation for Advanced Talents of Jiangsu University (13JDG071,12JDG054), Postdoctoral Science Foundation of China (2014M561577, 2014M561572) and Jiangsu Province Science and Technology Support Project (BE2014008 and BE2014008-2) for support.

Notes and references

[a] Automotive Engineering Research Institute, Jiangsu University, 301 Xuefu road, Zhenjiang 212013, P. R. China. E-mail: chenlong@ujs.edu.cn; Tel: +86 511-88780004

[b] Department of Chemistry and Key Laboratory of Advanced Energy Materials Chemistry (MOE), Nankai University, Tianjin 300071, P.R. China.

[c] Synergistic Innovation Center of Modern Agricultural Equipment and Technology, Jiangsu University, Zhenjiang 212013, P. R. China

[d] School of Material Science & Engineering, Center for Photon Manufacturing Science and Technology, Jiangsu University, Zhenjiang 212013, P. R. China. E-mail: wangyaping@ujs.edu.cn; Tel: +86 511 88797783

†Electronic supplementary information (ESI) available: X-ray crystallography, Tables S1 and S2, Fig. S1-S5, PXRD and TGA patterns. CCDC 1036655, 1036654 and 1023610 for **1-3**, respectively. For ESI and crystallographic data in CIF or other electronic format see DOI: 10.1039/c5cexxxxx.

1 (a) B. Chen, M. Eddaoudi, S.T. Hyde, M. O'Keeffe, and O.M. Yaghi, *Science,* 2001**,** 291, 1021; (b) B. Kesanli, Y. Cui, M. Smith, E. Bittner, B. Bockrath, and W. Lin, *Angew. Chem.,* 2005, 117, 74.

2 (a) X. B. Zhao, B. Xiao, A. J. Fletcher, K. M. Thomas, D. Bradshaw, and M. J. Rosseinsky, *Science,* 2004, 306, 1012; (b) P. Horcajada, C. Serre, M. Vallet-Regi, M. Sebban, F. Taulelle, and G. Férey, *Angew. Chem. In Ed.,* 2006, 45, 5974; (c) J.-R. Li, R. J. Kuppler, and H.-C. Zhou, *Chem. Soc. Rev.,* 2009, 38, 1477; (d) A. Demessence, D. M. D'Alessandro, M. L. Foo, and J. R. Long, *J. Am. Chem. Soc.,* 2009, 131, 8784.

3 (a) D. Maspoch, D. Ruiz-Molina, and J. Veciana, *Chem. Soc. Rev.,* 2007, 36, 770; (b) M. P. Suh, Y. E. Cheon, and E. Y. Lee, *Coord. Chem. Rev.,* 2008, 252, 1007; (d) B. Chen, S. Xiang, and G. Qian, *Acc. Chem. Res.,* 2010, 43, 1115; (e) Y. Cui, Y. Yue, G. Qian, and B. Chen, *Chem. Rev.,* 2012, 112, 1126.

4 (a) J. Y. Lee, O. K. Farha, J. Roberts, K. A. Scheidt, S. T. Nguyen, and J. T. Hupp, *Chem. Soc. Rev.,* 2009, 38, 1450; (b) A. Corma, H. García, and F. X. Llabrés i Xamena. *Chem. Rev.,* 2010, 110, 4606.

5 M. D. Allendorf, C. A. Bauer, R. K. Bhakta, and R. J. T. Houk, *Chem. Soc. Rev.,* 2009, 38, 1330.

6 (a) S. Yuan, Y.-K. Deng, and D. Sun, *Chem. Eur. J.,* 2014, 20, 10093; (b) H. Zhang, J. G. Ma, D. M. Chen, J. M. Zhou; S. W. Zhang, W. Shi, and P. Cheng, *J. Mater. Chem. C,* 2014, 2, 20450; (c) J. M. Zhou, W. Shi, H. M. Li, H. Li, and P. Cheng, *J. Phys. Chem. C*, 2014, 118, 416; (d) D. M. Chen, X. P. Zhang, W. Shi, and P. Cheng, *Cryst. Growth Des.,* 2014, 14, 6261.

7 (a) H. Li, Z. Niu, T. Han, Z. J. Zhang, W. Shi, and P. Cheng, *Sci. China. Chem.,* 2011, 54, 1423; (b) S. S. Nagarkar, A. K. Chaudhari, and S. K. Ghosh, *Cryst. Growth Des.,* 2012, 12, 572. (c) H. Li, W. Shi, K. N. Zhao, H. Li, Y. M. Bin, and P. Cheng, *Chem.-Eur. J.,* 2013, 19, 3358. (d) H. Li, W. Shi, N. Xu, T. Han, Z. Niu, Z. Chen, and P. Cheng, *Cryst. Growth Des.,* 2012, 12, 2602. (e) F.-N. Shin, D. Ananias, T.-H. Yang, and J.

Rocha, *J. Solid State Chem.,* 2013, 204, 321. (f) F.-N. Shi, M. L. Pinto, D. Ananias, and J. Rocha, *Microporous and Mesoporous Mater.,* 2014, 188, 172.

8 (a) H. Wang, S.-J. Liu, D. Tian, J.-M. Jia, and T.-L. Hu, *Cryst. Growth Des.,* 2012, 12, 3263; (b) F. Bu, Q. Lin, Q. Zhai, L. Wang, T. Wu, S. Zheng, X. Bu, and P. Feng, *Angew. Chem. Int. Ed.,* 2012, 51, 8538.

9 (a) D. Singh and C. M. Nagaraja, *Dalton Trans.,* 2014, 43, 17912; (b) K. S. Asha, P. R. Kavyasree, A. Georgea and S. Mandal, *Dalton Trans.,* 2015, 44, 1009.

10 (a) S. R. Batten, S. M. Neville, and D. R. Turner, Coordination Polymers: Design, Analysis and Application; Royal Society of Chemistry, Cambridge, 2008; (b) S. Hou, Q.-K. Liu, J.-P. Ma, and Y.-B. Dong, *Inorg. Chem.,* 2013, 52, 3225; (c) S. R. Halper, L. Do, J. R. Stork, and S. M. Cohen, *J. Am. Chem. Soc.,* 2006, 128, 15255. (d) A. Michaelides, and S. Skoulika, *Cryst. Growth Des.,* 2009, 9, 2039.

11 O. V. Dolomanov, L. J. Bourhis, R. J. Gildea, J. A. K.Howard, and H. Puschmann, 2009, *J. Appl. Cryst.,* 42, 339.

12 G. M. Sheldrick, (2008). *Acta Cryst.,* A64, 112.

13 A. L. Spek, *Acta Crystallogr., Sect. A: Found. Crystallogr.* 1990, 46, C34.

14 (a) V. A. Blatov, 2006. "Multipurpose crystallochemical analysis with the program package TOPOS" IUCr CompComm Newsletter 7, 4-38 available at http://iucrcomputing.ccp14.ac.uk/iucr-top/comm/ccom/newsletters/2006nov/; (b) V. A. Blatov, 2006, http://www.topos.ssu.samara.ru/starting.html.

15 (a) M. O’Keeffe, M. A. Peskov, S. J. Ramsden, and O. M. Yaghi, *Acc. Chem. Res.*, 2008, 41, 1782; (b) M. O’Keeffe, Reticular Chemistry Structure Resource (http://rcsr.anu.edu.au/).

16 (a) T.-T. Luo, H.-L. Tsai, S.-L. Yang, Y.-H. Liu, R. D. Yadav, C.-C. Su, C.-H. Ueng, L.-G. Lin, and K.-L. Lu, *Angew. Chem. Int. Ed.,* 2005, 44, 6063; (b) Q.-R. Fang, G.-S. Zhu, Z. Jin, M. Xue, X. Wei, D.-J. Wang, and S.-L. Qiu, *Angew. Chem.,* 2006, 118, 6272; (c) T.-W. Tseng, T.-T. Luo, S.-Y. Chen, C.-C. Su, K.-M. Chi, and K.-L. Lu, *Cryst. Growth Des.,* 2013, 13, 510; (d) X. Zhu, H. Zhang, Y. Luo, Y. Pang, and D. Tian, *Inorg. Chem. Commun.,* 2011, 14, 562; (e) A. B. Lysenko, E. V. Govor, and K. V. Domasevitch, *Inorg. Chim. Acta,* 2007, 360, 55.

17 H.-L. Gao, L. Yi, B. Zhao, X.-Q. Zhao, P. Cheng, D.-Z. Liao, and S.-P. Yan, *Inorg. Chem.,* 2006, 45, 5980; (b) Y.-X. Tan, Y.-P. He, and J. Zhang, *Chem. Commun.* 2014, 50, 6153. (c) M. Eddaoudi, J. Kim, N. Rosi, D. Vodak, J. Wachter, M. O’Keeffe, and O. M. Yaghi, *Science,* 2002, 295, 469. (d) J. He, J.-X. Zhang, G.-P. Tan, Y.-G. Yin, D. Zhang, and M.-H. Hu, *Cryst. Growth Des.* 2007, 7, 1508.

18 Y.-P. He, Y.-X. Tan, and J. Zhang, *Cryst. Growth Des.,* 2014, 14, 3493.

19 (a) D. L. Phillips, C. M. Che, K. H. Leung, Z. Mao, and M. C. Tse, *Chem. Rev.* 2005, 249, 1476. (b) E. Colacio, R. Kivekas, F. Lloret, M. Sunberg, J. Suarez-Varela, M. Bardaji, and A. Laguna, *Inorg. Chem.,* 2002, 41, 5141.

20 (a) R. H. Wang, D. Q. Yuan, F. L. Jiang, L. Han, Y. Q. Gong, and M. C. Hong, *Cryst. Growth Des.,* 2006, 6, 1351; (b) H. Wu, W. Dong, H. Y. Liu, J. F. Ma, S. L. Li, J. Yang, Y. Y. Liu, and Z. M. Su, *Dalton Trans.,* 2008, 5331.

21 J. Tao, J. X. Shi, M. L. Tong, X. X. Zhang, and X. M. Chen, *Inorg. Chem.,* 2001, *40*, 6328.

22 T. Ma, M.-X. Li, Z.-X. Wang, J.-C. Zhang, M. Shao, and X. He, *Cryst. Growth Des.,* 2014, 14, 4155.

23 (a) J.-R. Li, Y. Tao, Q. Yu and X.-H. Bu, *Chem. Commun.,* 2007, 1527; (b) Y.-W. Li, S.-J. Liu, T.-L. Hu, and X.-H. Bu, *Dalton Trans.,* 2014, 43, 11470; (c) H. He, F. Sun, T. Borjigin, N. Zhao, and G. Zhu, *Dalton Trans.,* 2014, 43, 3716.

24 (a) X. Zhao, X. Wang, S. Wang, J. Dou, P. Cui, Z. Chen, D. Sun, X. Wang, and D. Sun, *Cryst. Growth Des.,* 2012, 12, 2736; (b) L. Wen, L. Zhou, B. Zhang, X. Meng, H. Qua, and D. Li, *J. Mater. Chem.,* 2012, 22, 22603.

25 (a) Z. Jin, H. He, H. Zhao, T. Borjigin, F. Sun, D. Zhangc, and G. Zhu, *Dalton Trans.,* 2013, 42, 13335; (b) L. Hou, L.-N. Jia, W.-J. Shi, Y.-Y. Wang, B. Liu, and Q.-Z. Shi, *Dalton Trans.,* 2013, 42, 3653; (c) J.-J. Shen, M.-X. Li, Z.-X. Wang, C.-Y. Duan, S.-R. Zhu, and X. He, *Cryst. Growth Des.,* 2014, 14, 2818.

26 (a) E.-C. Yang, H.-K. Zhao, B. Ding, X.-G. Wang, and X.-J. Zhao, *Cryst. Growth Des.,* 2007, 7, 2009. (b) Y. Xu, F. Luo, Y.-X. Che and J.-M. Zheng, *Inorganic Chem. Commun.,* 2010, 13, 1489; (c) L. Dong, W. Chu, Q. Zhu, and R. Huang, *Cryst. Growth Des.,* 2011, 11, 93; (d) C. A. Bauer, T. V. Timofeeva, T. B. Settersten, B. D. Patterson, V. H. Liu, B. A. Simmons and M. D. Allendorf, *J. Am. Chem. Soc.,* 2007, 129, 7136.

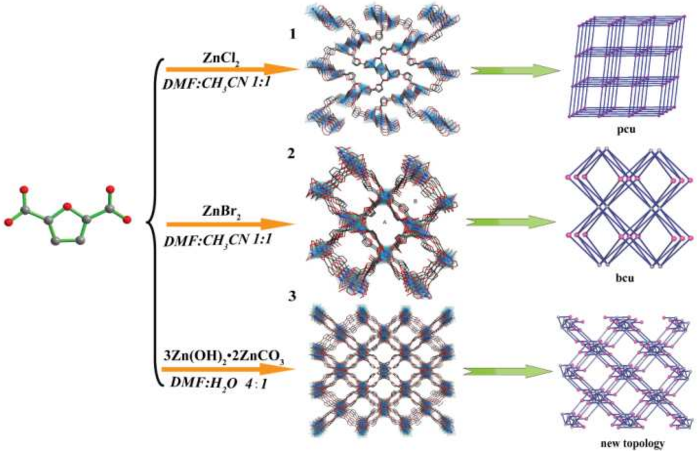

Topological controlled three noval metal-organic frameworks constructed from trinuclear zinc (II) building blocks based on furan-2,5-dicarboxylic acid were hydrothermally synthesized by anion adjusting and solvent tuning. And the blue luminescence of the Zn(II) complexes were investigated.